J. Fluid Mech. (1973), *vol.* 60, *part* 2, *pp.* 209–223
Printed in Great Britain

Shock attenuation in a 'gradual' area expansion

By M. A. NETTLETON
Central Electricity Research Laboratories, Leatherhead, Surrey

(Received 15 January 1973)

The effect of the angle of divergence ϕ, the magnitude of the area ratio A_{21} and the specific-heat ratio of the gas γ on the attenuation of a shock in a two-dimensional area expansion has been experimentally determined. The results are compared with current theories relating shock strength and area ratio. At some distance from the expansion the change in shock strength, for shocks with strengths up to 10, is predicted reasonably accurately by an analysis of Chisnell (1957). Close to the area change surprisingly strong shocks were observed. This is shown to result from the diffracted shock undergoing a Mach reflexion at the end of the expansion.

1. Introduction

Chisnell's (1957) extension of Chester's (1953, 1954) analysis of the change in shock strength in a gradual expansion has been incorporated in most treatments of shock attenuation. The resultant theories have been generalized and applied to expansions with angles of divergence ϕ between 5° and 90°. For instance, Whitham (1957, 1959) has used Chisnell's relationship between the shock strength Z (the pressure ratio across the shock) and area ratio in generalized theoretical treatments of two- and three-dimensional expansions. Davies & Guy (1969) have used the same relationship for the analysis of shock attenuation in an abrupt expansion. Deckker & Gururaja (1970) have examined experimentally the effect of the angle of divergence of the expansion on shock decay and concluded that Chisnell's analysis is unsatisfactory. Finally, Nettleton & Sloan (1973) have found that an empirical treatment of shock decay in three-dimensional expansions which incorporates the Chisnell analysis gives a reasonable description of their experimental results. Thus, it appears that an estimate of the range of applicability of the Chisnell result is required.

The essence of Chisnell's analysis is deceptively simple. Changes in strength across the shock front due to the area change are decoupled from changes in shock strength due to disturbances in the flow behind the shock. The strength of the front within the area change is non-uniform but can be assigned an average value. Subsequent to the area change Chester's (1953, 1954) analysis shows that this average strength is constant but local changes occur, resulting eventually in a shock of uniform strength. Chisnell showed that his solution is appropriate to converging cylindrical and spherical shocks. In these cases the accuracy is accounted for by the cancellation of reflected disturbances in the flow. These are due to (i) the interaction of the expansion wave and contact surface, (ii) the

propagation of the contact surface through the area change and (iii) the propagation of the expansion waves through the area change. By equating the pressures on either side of the contact surface formed between gas originally downstream and gas originally upstream of the area change in the equations for steady flow, Chisnell obtained the result

$$Af(Z) = \text{constant},$$

where A is the area and $f(Z)$ is a defined function of the specific-heat ratio γ and shock strength Z. When the area change is small and implicitly gradual the resultant shock strength is that of the uniform planar shock finally formed. Prior to this stage the resultant shock strength is considered to be the averaged value over the area of the shock front.

This is an idealized model of shock decay. As the planar shock reaches the diverging wall a portion diffracts round the corner taking up a constant strength, defined by the original strength, the wall angle and the specific-heat ratio. Expansion waves generated at the area change propagate towards the axis of symmetry, diminishing the area of planar shock of original strength. The angle α the head of these expansion waves make with the wall, and hence the distance travelled by the shrinking portion of the original shock, is a function of the original shock strength and the specific-heat ratio of the gas. A more detailed description of the processes occurring up to the crossing of the expansion waves is given by Skews (1967). The heads of the expansion waves interact at the axis of symmetry and the resultant waves further weaken the shock, starting from the axis of symmetry and eventually reaching the wall shock. Complex reflexion processes then occur at the walls, and the resultant waves eventually lead to the formation of a uniform shock. An estimate of the influence of these disturbances on the steady-state strength of the shock can be obtained from a comparison of the predictions of Chisnell's theory with those from Laporte's (1954) analysis of the change in shock strength in a sudden area change.

An additional complication arises at the end of the expansion when the walls become parallel. The wall shock meets a convergence and strengthens owing to a reflexion process. For small values of ϕ a Mach reflexion is produced. The reflexion travels inwards towards the axis of symmetry, re-strengthening the shock. A strong re-reflexion must occur at the axis of symmetry and the production of a resultant uniform shock is evidently a lengthy process. The shock strength averaging procedure required to produce a value of strength to compare with the Chisnell value is evidently an extremely complex process. Furthermore, the only simple and obvious definition of a 'gradual' area change appears to lie in a relationship between the angle of divergence and the angle the expansion wave heads make with the channel wall. Thus, for small values of ϕ and large values of α the shock weakening processes should produce a uniform shock in a short length of channel and the subsequent strengthening via Mach reflexions should be minimized.

The present experiments in two-dimensional expansions with different angles of divergence, different area ratios, gases with $\gamma = 1{\cdot}67$ and $1{\cdot}40$ resulting in different values for α and with shocks of various strengths have been carried out in an attempt to resolve these difficulties.

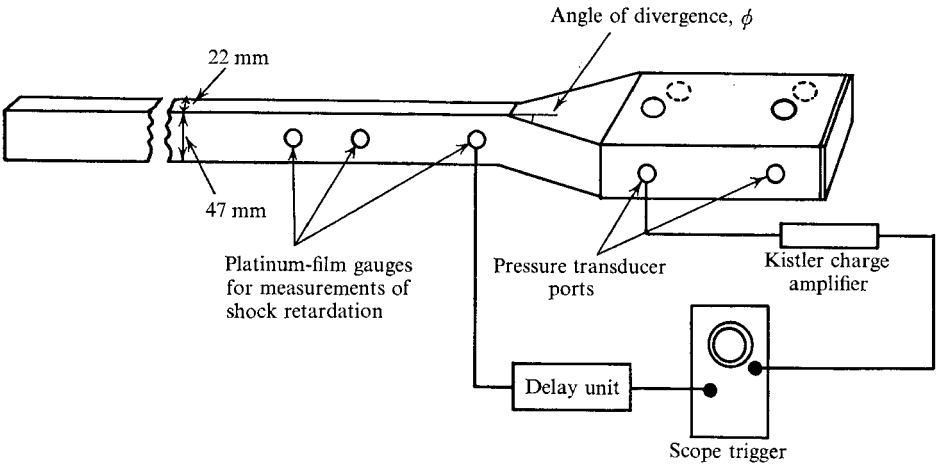

FIGURE 1. Sketch of the apparatus.

2. Experiments

The experiments were performed in expansion sections connected to the test section of a rectangular shock tube previously described by Nettleton & Sloan (1971). The experimental arrangement is shown in figure 1. Two channels 47×47 mm and 47×109 mm were constructed to give area ratios of 2·14 and 4·95 respectively. These were connected to the 22×47 mm shock tube by straight-sided sections of various lengths so that the 22 mm sides increased to 47 or 109 mm. Both the test section of the tube and the final parallel-sided section were equipped with instrument ports to allow measurements of shock velocities and pressures. Pressures were generally measured with Kistler 601 B acceleration-compensated gauges, amplified by Kistler 5001 amplifiers and displayed on a Tektronix 556 oscilloscope. The oscilloscope time base was normally $10\,\mu s\,cm^{-1}$ and shock pressures were taken as the amplitude $5\,\mu s$ after the initial rise, which generally corresponded to the maximum amplitude. Duplicate measurements were made at symmetrical positions on opposing sides in each experiment and the estimated accuracy in pressure measurement was $\pm 5\,\%$. Helium and air were used as the driver gases and air and argon as the test gases.

3. Results

3.1. *General features*

In general the strength Z_{red} of the wall shock was measured in the parallel-sided channel following the expansion section close to and some distance from the area change. These measurements are plotted in terms of the strength Z_{inc} of the shock incident upon the area change, making appropriate allowance for the attenuation of the shock between the final film gauge and the entrance to the area change. Shock attenuation was significant with $Z_{inc} > 7$. Each measurement is the mean of results at directly opposite stations and the vertical bars in the plots represent the spread of the results. Figure 2 shows two typical traces from opposite stations

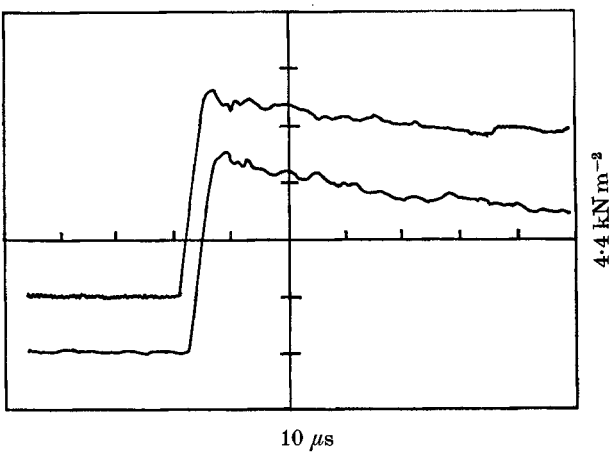

FIGURE 2. Typical experimental records from opposite pressure transducers in the expanding wall close to the area change. $\phi = 15°$, $A_{21} = 4{\cdot}95$, $\gamma = \frac{5}{3}$, $M_s = 3{\cdot}77$, $Z_{\text{inc}} = 17{\cdot}53$ and $Z_{\text{red}} = 12{\cdot}6$ and $12{\cdot}9$.

with an oscilloscope time base of $10\,\mu$s per division. Shock strengths were measured from the amplitude of the trace $5\,\mu$s after the first rise. In general the reproducibility is about $\pm 5\,\%$, deteriorating somewhat for the stronger shocks, $Z > 12$.

3.2. *Influence of the angle of divergence* ϕ

Figures 3–7 show the experimental results for the strengths Z_{red} of the shock transmitted through the area change for a range of strengths Z_{inc} of the shock incident upon the area change. The results are for shocks in a gas with $\gamma = \frac{7}{5}$ for $\phi = 1{\cdot}5°$, $5°$, $10°$, $15°$ and $90°$ and are generally for the shock strength on the diverging wall. However, figure 6 shows for comparison some measurements of the strength made close to the area change on the non-divergent walls.

The results from two of the available theoretical treatments of shock attenuation in an area expansion are shown in figures 3–6. The full lines show the predictions from Chisnell's theory for the two area ratios. The dotted lines are the predictions from a steady-state approach to the problem, similar to that outlined by Laporte (1954) and Chester (1960). The present results have been obtained following a procedure given by Rudinger (1969, p. 163) for computing the interaction of a shock wave with a sudden area change. For incident shock strengths greater than 5, such solutions consist of a weakened shock transmitted downstream (Z_{red}). This shock is accompanied by a further shock which is formed in the area change and which is swept downstream by the flow. It is also possible to calculate the strength of the transmitted shock from Whitham's (1957) theory for the weakening of a shock at a convex corner according to the equation

$$\phi = \int_{M_0}^{M_w} \frac{dM}{Ac}, \tag{1}$$

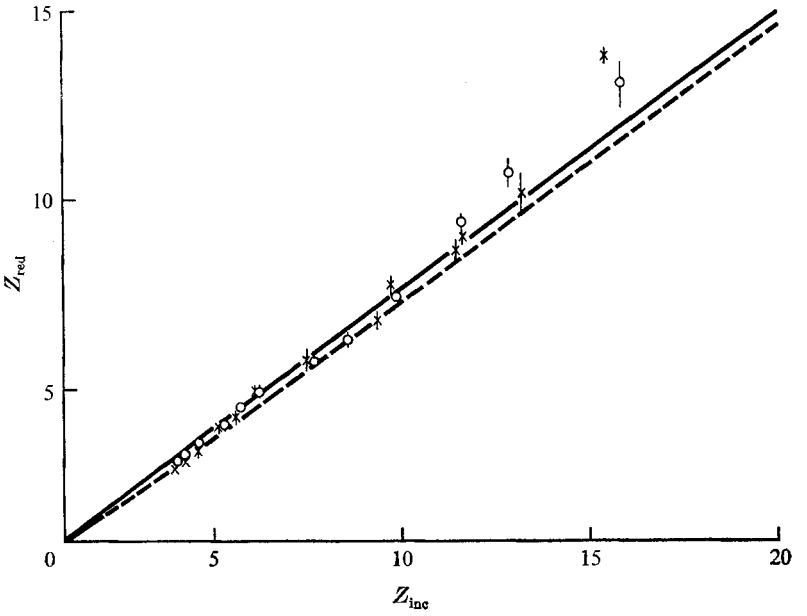

FIGURE 3. Influence of the angle of divergence. $\phi = 15°$, $\gamma = \frac{7}{5}$, $A_{21} = 2{\cdot}14$. ——, Chisnell; – –, steady state; ○, 0·8 diameters from area change; ×, 5·6 diameters.

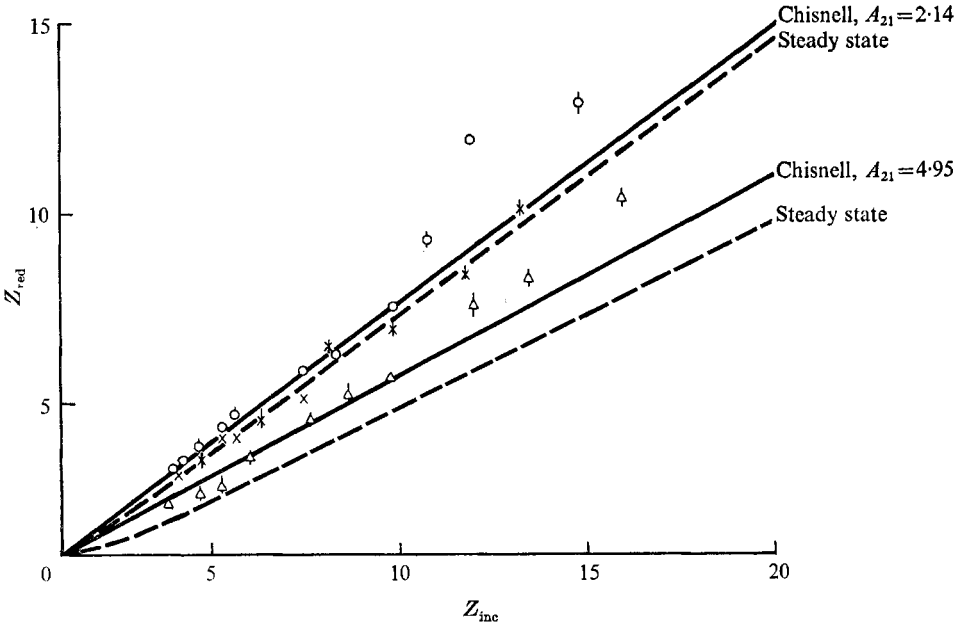

FIGURE 4. Influence of the angle of divergence. $\phi = 5°$, $\gamma = \frac{7}{5}$. ○, 0·8 diameters from area change, $A_{21} = 2{\cdot}14$; ×, 0·6 diameters, $A_{21} = 4{\cdot}95$.

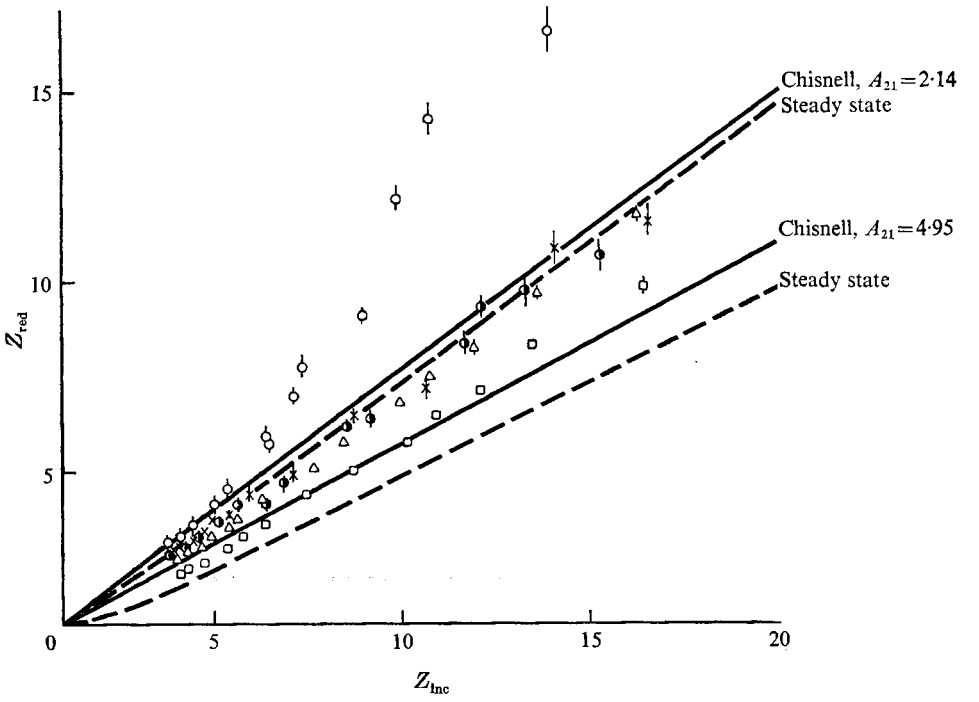

FIGURE 5. Influence of the angle of divergence. $\phi = 10°, \gamma = \frac{7}{5}$. ○, 0·8 diameters from area change, $A_{21} = 2{\cdot}14$; □, 5·6 diameters, $A_{21} = 2{\cdot}14$; △, 0·6 diameters, $A_{21} = 4{\cdot}95$; ×, 7·1 diameters, $A_{21} = 4{\cdot}95$.

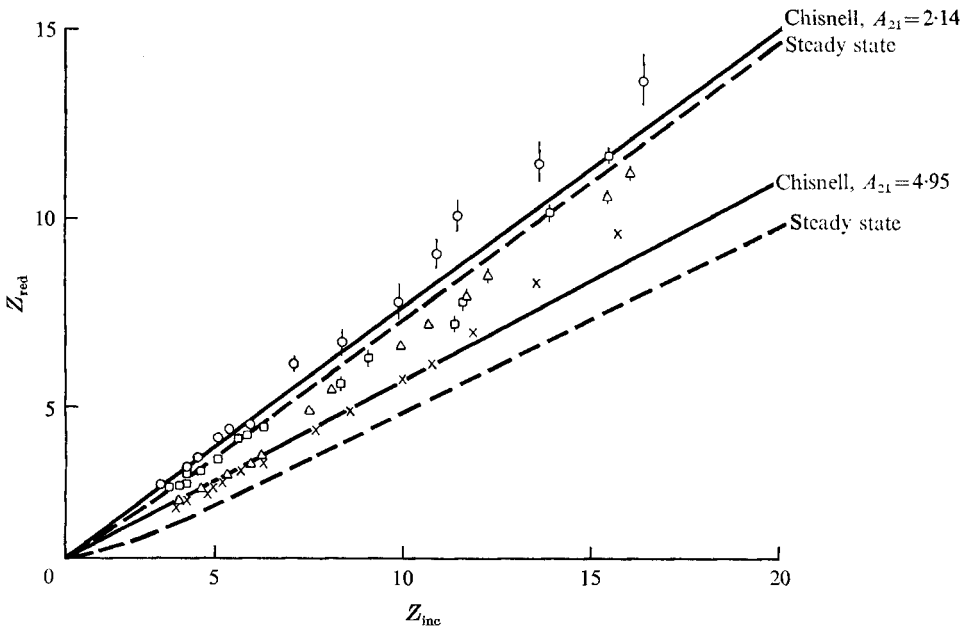

FIGURE 6. Influence of the angle of divergence. $\phi = 15°, \gamma = \frac{7}{5}$. Divergent walls: ○, 0·8 diameters from area change, $A_{21} = 2{\cdot}14$; ×, 5·6 diameters, $A_{21} = 2{\cdot}14$; △, 0·6 diameters, $A_{21} = 4{\cdot}95$; □, 7·1 diameters, $A_{21} = 4{\cdot}95$. Non-divergent walls: ◑, 0·8 diameters, $A_{21} = 2{\cdot}14$.

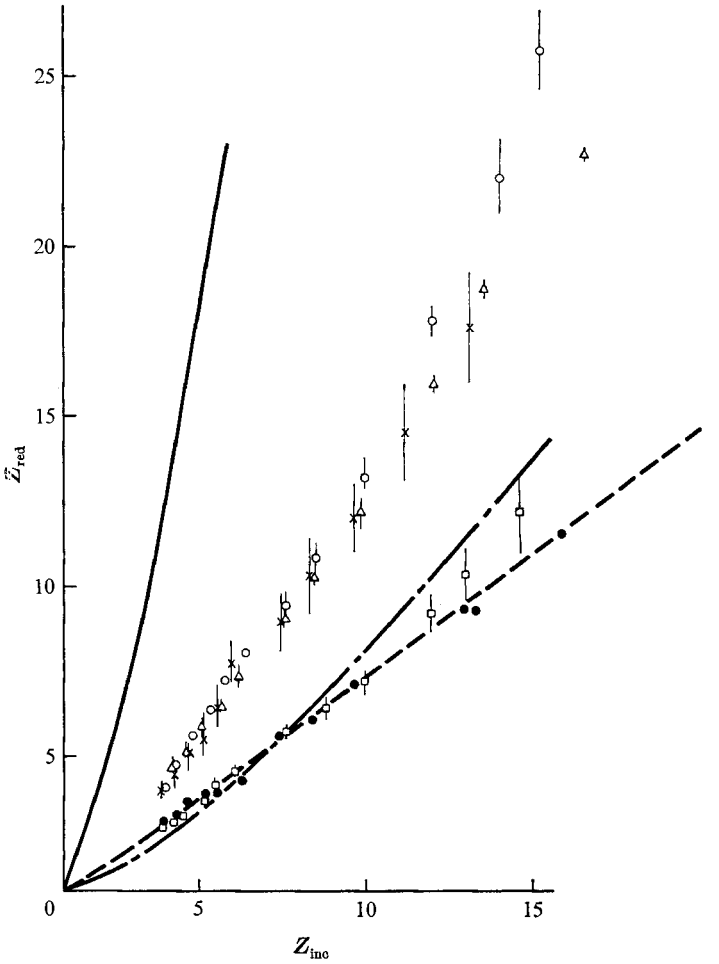

FIGURE 7. Influence of the angle of divergence. $\phi = 90°$, $\gamma = \frac{7}{5}$, $A_{21} = 2{\cdot}14$. Curved walls, 0·8 diameters from area change: ○, $r = 3{\cdot}02$ cm; △, $r = 4{\cdot}76$ cm. Parallel walls, 5·6 diameters: ×, $\phi = 90°$; □, $\phi = 90°$, expanding wall; ●, straight wall. ——, reflexion of Z_{inc}; – · –, reflexion of Skew's wall shock; – –, steady state.

followed by its strengthening at a concave corner according to the equation

$$\cot\phi = \frac{M_0(1 + A_w M_w / A_0 M_0)}{M_w\{(1 - M_0^2/M_w^2)(1 - A_w^2/A_0^2)\}^{\frac{1}{2}}}. \tag{2}$$

In these equations the subscript 0 refers to conditions before the change in direction ϕ and the subscript w to conditions after the corner, M is the Mach number of the flow, A is the ray area and

$$c = \{-d(M^2)/d(A^2)\}^{\frac{1}{2}}. \tag{3}$$

The resulting predictions for $\phi \leqslant 15°$ are adequately represented by a line of gradient 45° through the point (1, 1) on the plots. Increasing the shock strength and the angle ϕ leads to small departures from the condition $Z_{inc} = Z_{red}$. For

instance, with $\phi = 15°$ and $Z_{\text{inc}} = 10{\cdot}47$ the shock weakens to give $Z_{\text{red}} = 8{\cdot}34$ at a convex corner and a shock of this strength intensifies to a strength 10·68 at the concave corner at the exit from the area change. Thus the maximum departure from the condition $Z_{\text{inc}} = Z_{\text{red}}$ does not exceed 2 %.

A comparison of the experimental results with predictions from the three theoretical treatments is probably most readily described in terms of increasing values of ϕ for $\phi \leqslant 15°$. For the smaller area change $A_{21} = 2{\cdot}14$, there is little difference between the predictions from Chisnell's analysis and from the steady-state treatment. However, with $\phi \geqslant 10°$ the steady-state treatment is probably slightly superior for predictions at the position furthest from the area change. Close to the area change Chisnell's theory is in good agreement with the experimental results for $\phi \leqslant 10°$ and for shocks with $Z_{\text{inc}} \leqslant 10$. For stronger shocks the experimental results are considerably higher than those Chisnell's theory would predict and the discrepancy between theory and experiment increases with increasing values of ϕ. Indeed for $\phi = 15°$ the experimental results close to the area change approach the theoretical result $Z_{\text{inc}} = Z_{\text{red}}$ obtained from Whitham's analysis. For the larger area change $A_{21} = 4{\cdot}95$, the steady-state model leads to transmitted shock strengths significantly lower than those predicted from Chisnell's analysis. In turn, Chisnell's analysis in general underestimates the experimental results. Close to the area change the Chisnell theory is in close agreement with measured shock strengths for values of $Z_{\text{inc}} \leqslant 6$, with the discrepancy between theory and experiment increasing with increasing values of Z_{inc} and ϕ. Further from the area change the Chisnell theory is very satisfactory for shocks of strength up to 10 and reasonably good for incident shock strengths between 10 and 15. Finally, the results for the shock strength on the non-divergent walls close to the area change shown in figure 6 are in close agreement with those measured at some distance from the area change on the divergent walls. Thus the results for the non-divergent walls are adequately represented by the Chisnell analysis and probably rather better by the steady-state treatment.

The results for the divergent wall with $\phi = 90°$ (figure 7) consist of three sets of measurements from close to the area change; one set was obtained with a 90° corner and the other two sets with curved transition pieces, radii 305 and 476 mm, fixed in the corner in an attempt to produce a gradual area change. The results show that the attempted rounding-off of this corner had little or no effect on the shock strength. Furthermore, the results depart markedly from the theory developed for a gradual area change. More surprisingly, the results some distance from the area change are in reasonable agreement with the Chisnell and steady-state theories. In addition the similarity in the shock strength on the non-divergent and expanding wall suggests that the shock has become planar again some five diameters from the area change although substantial differences were confirmed between the strengths of the shock on the straight and divergent walls 0·6 diameters from the area change. Thus a set of results for the straight wall but from close to the area change were so similar to the results 5·6 diameters away that they could not be readily included in figure 7. Also shown on figure 7 are lines representing normal reflexion of the incident shock and normal reflexion of a wall

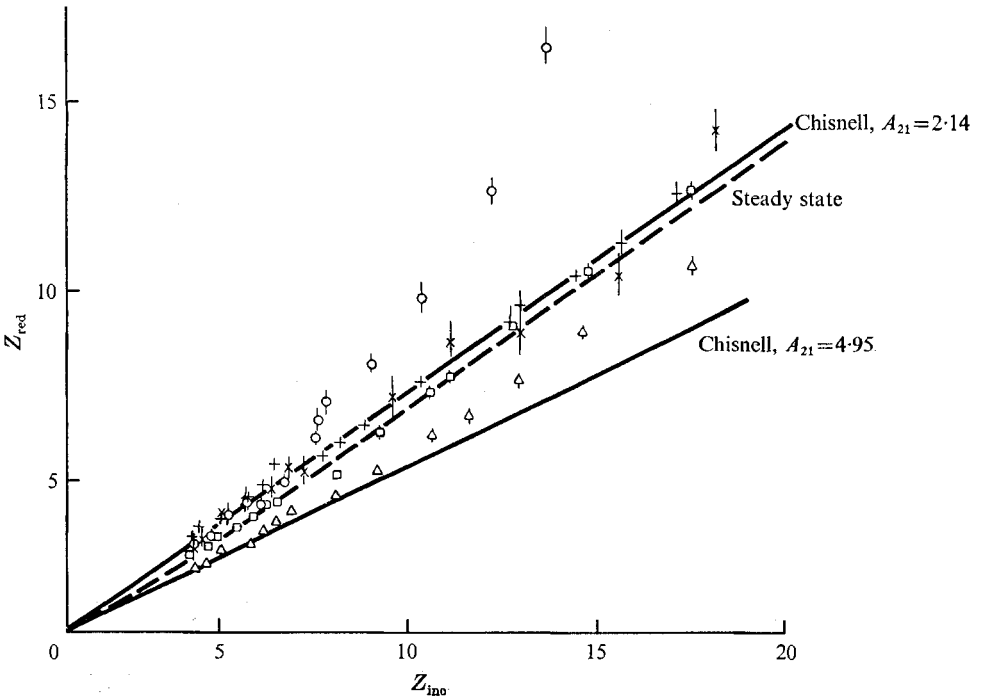

FIGURE 8. Influence of γ on shock decay and decay in a parallel-sided expanded channel. $\phi = 15°$, $\gamma = \frac{5}{3}$. $A_{21} = 2{\cdot}14$: ○, 0·8 diameters from area change; ×, 5·6 diameters; +, 3·2 diameters. $A_{21} = 4{\cdot}95$: □, 0·6 diameters; △, 7·1 diameters.

shock of the strength given by Skews (1966) for an angle of divergence of 90°. These will be commented upon in the subsequent discussion.

Similar results were obtained for the same range of values of ϕ with shocks in a gas with $\gamma = \frac{5}{3}$. Figure 8 shows a set of results for $\phi = 15°$. In this case the Chisnell and steady-state treatments underestimate the shock strength close to an area change of 2·14 but are reasonably accurate some distance away. However, with a larger area change the theory markedly underestimates the shock strength close to the area change and with $Z_{inc} \geqslant 10$ also at some distance from the area change; for weaker shocks the theory is satisfactory at a distance from the area change.

3.3. *Decay of shock in the exit channel*

Figure 8 includes results for three positions in the parallel-sided channel, following an area change of 2·14. In terms of the hydraulic diameter of the expanded channel these were 0·8, 3·2 and 5·6 diameters from the area change. It is apparent from figure 8 that most of the shock decay takes place shortly after the area change and that there is only a small decrease in shock strength between 3·2 and 5·6 diameters from the end of the area change.

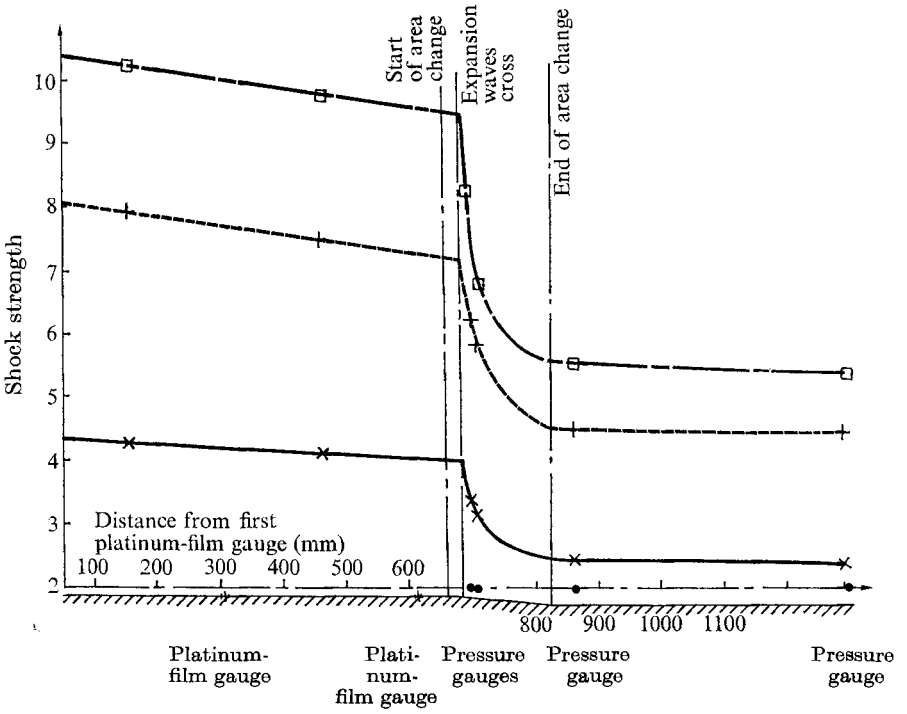

FIGURE 9. Decay of shock within the expansion. $\phi = 15°$, $\gamma = \frac{7}{5}$, $A_{21} = 4{\cdot}95$.

3.4. *Decay of shock in the area change*

Figure 9 shows the decline in shock strength on the non-expanding walls along the axis of symmetry for shocks of strength 9·5, 7·2 and 4·0 incident on the area change of 4·95 with $\phi = 15°$. The origin of the abscissa is the first platinum film gauge and the first two points for each shock strength are determined from the Mach numbers measured between film gauges 1 and 2 and film gauges 2 and 3. The plot is drawn assuming a linear fall in shock strength to the point where the expansion waves, originating from the start of the area change, cross at the axis of symmetry. There are two measurements within the area change showing the rapid decay there and two subsequent measurements in the expanded channel. The plot is drawn by extrapolating the later results back to the exit of the area change, thus assuming that most of the attenuation occurs within the area change.

3.5. *Measurements of shock curvature in the exit channel*

Attempts were made to determine the shock curvature at the start and the end of the final channel following an expansion section with $\phi = 15°$ for the experiments at the inlet of the final channel and $\phi = 10°$ for experiments at the end of the final channel with $A_{21} = 2{\cdot}14$ in both cases. The results from the beginning of the channel were not wholly conclusive: ten measurements of the time of shock transit from the start of the area change to a gauge in the non-divergent wall gave $85{\cdot}5 \pm 2\,\mu$s and a further ten measurements with similar shock strengths

for the divergent walls gave $86{\cdot}5 \pm 2\,\mu$s. Converting the transit times to velocities leads to a mean shock velocity of $1{\cdot}00\,\text{mm}/\mu\text{s}$ along the straight wall and $1{\cdot}01\,\text{mm}/\mu\text{s}$ along the divergent wall. The higher velocity along the divergent wall results from the longer distance travelled. These velocities result in a shock bowed out in the direction of travel by 0·8 mm after $100\,\mu$s. At the end of the channel shock velocities were obtained from measurements of the shock strength close to the end face. Thus the time of arrival at the end face could be predicted from the shock velocity derived from the shock strength and the known distance between the gauge and end face. Six runs with shocks of strength 10 gave times of arrival at the end face $2{\cdot}8 \pm 0{\cdot}3\,\mu$s greater than those predicted from the measured shock strength. Allowing for the rise time of the end wall gauge and associated recording instrumentation, $2\,\mu$s, the curvature is similar in magnitude to that at the start of the channel but is reversed in direction.

4. Discussion

Measurements of the ratio of the strength of the shock propagating along the diverging wall to that of the shock on the straight wall offer some degree of discrimination between the two types of theory describing the attenuation of a shock in an expanding channel. Thus, the Chisnell and steady-state flow relationships imply minimal differences in shock strength across its periphery and rapid equilibration of such differences. In contrast, the Whitham–Skews analysis emphasizes the differences between the shock propagating along the straight and divergent walls, especially in the early stages. The differences in strength are shown to be greatest for strong shocks and large values of ϕ. Furthermore, on the basis of the later theory it is possible to specify the length of the area change along which the initial difference is maintained between the strength of the straight- (Z_{inc}) and divergent-wall shocks. The straight-wall shock cannot decay until the expansion waves from the inlet to the area change cross at the axis of symmetry. Skews (1967) has given a derivation of the angle α the heads of the expansion waves make with the original channel wall, namely

$$\tan\alpha = \frac{(\gamma-1)\,(M_{\text{inc}}^2-1)\,\{M_{\text{inc}}^2+[2/(\gamma-1)]}{(\gamma+1)\,M_{\text{inc}}^4}, \tag{4}$$

where γ is the ratio of specific heats. The value of α rises rapidly with increasing values of the incident shock strength to an approximately constant value; for $M_{\text{inc}} \geqslant 1{\cdot}2$ the value lies between 25° and 28° for $\gamma = \frac{7}{5}$. With $\tan\alpha = 0{\cdot}5$ ($\alpha = 26{\cdot}6°$) and the radius r of the smaller channel 11 mm, the smaller dimension of the channel used in the present experiments, the expansion heads cross 22 mm from the inlet into the area change. Thus, the theory predicts the maintenance of differences in shock strength for significant penetrations ($x = r/\tan\alpha \sim R$, the larger dimension of the initial channel in the present experiments) into the area change.

The position at which the heads of the expansion fans cross is also a useful indication of the distance travelled by the divergent-wall shock, before it is weakened by the refracted expansion waves. The length e of the area change must

be significantly greater than $r/\tan\alpha$, say $e \geqslant 3r/\tan\alpha$, before the strength of the divergent-wall shock which is incident on the concave corner at the end of the area change is reduced below the Skews–Whitham prediction. The criterion for the maximum length of area change for constant shock strength is a complex function of the incident shock strength, rate of shock decay and ϕ. The empirical relationship presently suggested is shown to discriminate between the area ratios investigated. For shorter area changes, the Skews–Whitham theory indicates that the strength of the shock reaching the concave corner depends on ϕ and the strength of the original shock but not on the area ratio. It will be recalled that in the previous section it was shown that the Whitham analysis of shock decay at a convex corner followed by intensification at a concave corner produced little change in shock strength ($< 2\,\%$). This was based on the strength of the divergent-wall shock remaining constant at the value predicted from (1) until it reached the concave corner. It appears that expansion sections with $e < 3r/\tan\alpha$ satisfy these conditions and such sections should result in $Z_{\text{inc}} = Z_{\text{red}}$.

Let us compare experiment and theory starting at a distance from the area change and working downstream to within the area change. For values of $\phi \leqslant 15°$ and for incident shock strengths less than 10, the steady-state theory is in close agreement with the experimental results for area ratios of 2·14, whilst the Chisnell analysis gives more satisfactory agreement for the larger area ratio. However, the difference between the steady-state and Chisnell analysis is slight for the smaller area ratio. The divergent-wall shock is much stronger than is predicted in the larger area ratio for $Z_{\text{inc}} \geqslant 10$, although even the strongest shocks have almost reached equilibrium some 6 diameters from the exit of the smaller area ratio. This is not unexpected since equilibration of the shock is evidently a lengthy process. Thus evidence of slight shock curvature could still be detected at the end of the channel with $A_{21} = 2{\cdot}14$. Furthermore, figure 8 suggests that the rate of equilibration of the shock strength falls with increasing distance from the exit of the area change. The contrast in results for shocks with $Z_{\text{inc}} \geqslant 10$ can be accounted for in terms of the longer lateral distances which the perturbations equalizing the pressure across the shock periphery must travel for the larger area ratio.

There is no evidence in the results for values of $\phi \leqslant 15°$ from close to the area change of Z_{red} becoming independent of the area ratio as suggested earlier. However, the experimental results for $A_{21} = 2{\cdot}14$ and $\phi = 15°$ imply that the divergent-wall shock does not weaken from the Skews–Whitham value before it impinges on the convergent corner. The implication is drawn from the fair description of the experimental results for Z_{red} *vs.* Z_{inc} in figures 6 and 8 by a line of gradient 45°. For $A_{12} = 4{\cdot}95$, $e = 162{\cdot}3$ mm and for $A_{12} = 2{\cdot}14$, $e = 46{\cdot}7$, and the empirical criterion suggested for the length of area change required for significant weakening of the divergent-wall shock ($e \geqslant 3r/\tan\alpha$) is $e \geqslant 66$ mm. Thus the criterion satisfactorily discriminates between the present results.

Increasing the value of ϕ from 15° to 90° does not prevent almost complete equilibration of the shock strength, as measured by the agreement between experiment and steady-state theory, 5·6 diameters from the area change. However, the results for the divergent wall close to the area change indicate that

	Gauge closest to expansion inlet		Gauge downstream of inlet	
Z_{inc}	Measured Z	Chisnell's Z	Measured Z	Chisnell's Z
4·0	3·4	3·5	3·1	3·2
7·2	6·2	6·3	5·8	5·6
9·5	8·3	8·3	6·9	7·2

TABLE 1. Comparison of predictions from $Af(Z)$ = constant with experimental results from the non-divergent wall of the area change

modifications to the abruptness of the area change have little effect on the rate at which the shock becomes uniform. For comparison there are included on figure 7 lines representing possible upper and lower limits for the shock strength at the start of the expanded channel. The upper limit is based on full reflexion of the incident shock. Since the incident strength only exists across a decreasing area, centred on the axis of symmetry and travelling along it, the upper limit should be a generous overestimate. The lower limit is based on the strength of a reflexion of the wall shock measured by Skews (1967) for a 90° corner. This should give an accurate estimate of the lower limit which should occur at the corner in the second channel. The shock periphery striking the measuring station 0·8 diameters from the corner will not be normal to the wall. In addition, further difficulties arise in considering the effect of the reflected shock propagating away from the outer corner across the shock periphery, when attempting to compare the pressure at the 0·8 diameter measuring station with the value at the corner. The wide discrepancy between the experimental results and the lower limit predictions indicate that effects such as these must be important.

Table 1 shows the merits of Chisnell's analysis when applied to predictions of the shock strength along the straight wall, within the area change. It is based on the use of the ratio of the channel area at the measuring station to that at the inlet of the expansion in Chisnell's $Af(Z)$ relationship. The agreement between measurements and predictions at the first gauge is particularly good, indicating that the non-divergent-wall shock rapidly attains the Chisnell average value following the crossing of the heads of the expansion waves at the axis of symmetry.

Finally table 2 gives an indication of how the shock strength averages out during its travel through the channel at the exit from the area change. The experimental results come from figures 6 and 9, the Mach reflexion result from Chisnell's predictions for an area ratio of 4·95 in combination with equation (2) and the Skews wall shock from Whitham's equation, equation (1) in the present text. As is the case within the area change Chisnell's theory adequately describes the experimental results from the non-divergent wall at both stations. The agreement with theory is possibly slightly better for the divergent wall at the station farthest from the area change. Close to the area change the experimental results are in general higher than the theory indicates. In terms of the Chisnell theory averaging out in shock strength is occurring via the weakening of the shock periphery close to the divergent walls. In this context the high

Z_{inc}	Measured strength close to the area change: Non-divergent wall	Measured strength close to the area change: Divergent wall	Chisnell's prediction	Mach reflexion of Chisnell's prediction according to (2)	Skews' wall shock	Measured strength far from area change: Non-divergent wall	Measured strength far from area change: Divergent wall
4·0	2·3	2·6	2·5	3·0	3·2	2·3	2·4
7·2	4·4	4·9	4·2	5·3	5·5	4·4	4·2
9·5	5·6	6·6	5·3	6·5	7·7	5·5	5·3

TABLE 2. Equilibration of the shock in the final channel

experimental values of the shock strength on the divergent wall can be compared with the results in column 5 of table 2. These results are based on the assumption that the shock has equilibrated in travelling through the expansion but is strengthened via a reflexion at the concave corner at the end of the expansion according to Whitham's theory given by (2). The values obtained in this way are in reasonable agreement with the experimental results. Column 6 shows that the Skews–Whitham treatment considerably overestimates the strength of the divergent-wall shock close to the area change.

5. Conclusions

(i) Chisnell's relationship between the shock strength and channel area produces tolerable predictions of the shock strength at some distance from a two-dimensional area change for shocks of strength less than 10, in gases with $\gamma = \frac{7}{5}$ and $\frac{5}{3}$.

(ii) Close to the area change the Skews–Whitham analysis of diffraction can be applied to account for the occurrence there of surprisingly strong shocks.

(iii) Shock strengths close to an area change with an angle of divergence of 90° are not affected significantly by using curved walls to temper the change.

(iv) The shock strength along the axis of symmetry within an area change falls off very rapidly. For a divergent wall with $\phi = 15°$ it drops to about half the value for the shock incident on the area change within 25 mm of the point at which the expansion waves cross.

The author is grateful to R. Cannon for his assistance in the experimental work. The work was carried out at the Central Electricity Research Laboratories and the paper is published by permission of the Central Electricity Generating Board.

REFERENCES

CHESTER, W. 1953 *Quart. J. Mech. Appl. Math.* **6**, 440.

CHESTER, W. 1954 *Phil. Mag.* **45**, 1293.

CHESTER, W. 1960 *Adv. in Appl. Mech.* **6**, 119.

CHISNELL, R. F. 1957 *J. Fluid Mech.* **2**, 286.

DAVIES, P. O. A. L. & GUY, T. B. 1971 *Symposium on Internal Flows, University of Salford*, paper 30, p. D46.

DECKKER, B. E. L. & GURURAJA, J. 1970 *Thermodynamics and Fluid Mechanics Convention, University of Glasgow*, p. 27. London: Inst. Mech. Engrs.

LAPORTE, O. 1954 *Los Alamos Sci. Lab. Rep.* LA 1740.

NETTLETON, M. A. & SLOAN, S. A. 1971 *Shock Tube Research, Proc. 8th Int. Shock Tube Symp.*, paper 18. Chapman & Hall.

NETTLETON, M. A. & SLOAN, S. A. 1973. To be published.

RUDINGER, G. 1969 *Nonsteady Duct Flow: Wave-Diagram Analysis.* Dover.

SKEWS, B. W. 1966 *University of Witwaterstand, Dept. Mech. Engng Rep.* no. 35.

SKEWS, B. W. 1967 *J. Fluid Mech.* **28**, 297.

WHITHAM, G. B. 1957 *J. Fluid Mech.* **2**, 145.

WHITHAM, G. B. 1959 *J. Fluid Mech.* **5**, 369.